LETTER TO THE EDITOR

The effect of non-axisymmetric wall geometry on ^{13}C transport in ASDEX Upgrade

J. Miettunen[1], T. Kurki-Suonio[1], T. Makkonen[1], M. Groth[1], A. Hakola[2], E. Hirvijoki[1], K. Krieger[3], J. Likonen[2], S. Äkäslompolo[1] and the ASDEX Upgrade Team

[1] Department of Applied Physics, Aalto University, Association Euratom-Tekes, PO Box 14100, FI-00076 AALTO, Finland

[2] VTT, Association Euratom-Tekes, PO Box 1000, FI-02044 VTT, Finland

[3] Max-Planck-Institut für Plasmaphysik, EURATOM Association, Boltzmannstrasse 2, D-85748 Garching, Germany

E-mail: juho.miettunen@aalto.fi

Abstract. We present first results of 3D simulations of global ^{13}C transport in ASDEX Upgrade (AUG) indicating that the deposition profile of ^{13}C exhibits toroidal asymmetry in the main chamber.

In 2007, the migration of carbon in AUG was studied with a methane ($^{13}CH_4$) injection experiment [1]. The total amount of deposited ^{13}C was estimated by assuming toroidally symmetric deposition. Remarkably, the total number of deposited atoms was observed to be less than 10 % of the number of injected atoms.

The experiment has been simulated with the 3D orbit-following Monte Carlo code ASCOT using both a realistic 3D wall geometry of AUG and a 3D magnetic field with toroidal ripple. The simulations indicate that the non-axisymmetric wall geometry causes notable toroidal asymmetry in the deposition profile in the outer (low-field side) midplane region which can provide a partial explanation for the missing carbon inferred from post-mortem analysis of ^{13}C deposition.

PACS numbers: 52.55.Fa, 52.65.Pp, 52.40.Hf, 52.25.Fi, 52.25.Vy

In the initial phase of ITER, carbon in the form of carbon-fibre-composite (CFC) has been foreseen to be used in the strike-point regions of the divertor [2]. The migration of carbon impurities in tokamak plasmas has been widely studied with trace-element injection experiments, see, e.g., [1, 3, 4]. These studies help to identify net erosion and deposition zones and also improve the understanding of the underlying physics related to impurity transport in general.

ASDEX Upgrade provides an interesting environment for impurity migration studies after being transformed into a full-tungsten tokamak. At the end of the 2007 experimental campaign in AUG, isotopically labelled methane in the form of $^{13}CH_4$ was injected into the torus from one valve at the outer midplane (located radially approximately 1.2 m away from the closest wall tiles) during successive low-density L-mode discharges #22573–#22585. For these discharges, done in deuterium, global plasma parameters were the following: toroidal magnetic field $B_t = -2.5$ T, plasma current $I_p = 0.8$ MA with the ion $\mathbf{B} \times \nabla B$ drift pointing towards the lower divertor, line-averaged electron density $n_e = 3.3 \cdot 10^{19}$ 1/m^3 and external heating by ECRH of $P_{aux} = 0.9$ MW. For studying the effect of substrate material on the migration of carbon, one poloidal set of the divertor tiles, the marker tiles, was left with a carbon stripe. To minimize erosion of deposited ^{13}C, the experiment was carried out during the last day of the campaign.

After the discharges the marker tiles as well as selected tungsten-coated tiles were removed for post-mortem analysis. Toroidally, the tiles were located in sector 11 approximately 45° away from the injection valve in sector 9, except for one limiter tile which was removed from sector 8 next to the valve. Poloidally, the divertor tiles formed a complete set, whereas regarding the main chamber three tiles were removed from the central column heat shield together with single tiles from the top of the vessel, upper passive stabilizer loop and outer midplane limiter. Carbon deposition on samples from the removed tiles was analyzed using secondary ion mass spectrometry (SIMS). As only central parts of the tiles were available for analysis, possible carbon deposition in gaps between adjacent tiles was not assessed.

With the assumption of toroidally symmetric deposition, the total amount of deposited ^{13}C was calculated by integrating the measured deposition in the poloidal and toroidal directions over the entire torus. Remarkably, the integrated ^{13}C deposition on the divertor tiles was observed to be less than 1.5 % of the number of injected ^{13}C atoms. The main chamber measurements are more uncertain due to the small number of removed tiles. The total ^{13}C deposition on the main chamber tiles and remote areas such as below the divertor roof baffle was estimated to be in the range of 3–8 % of injected ^{13}C. Thus, the total ^{13}C deposition in the entire torus was calculated to be approximately only 4.5–9.5 % of the number of injected ^{13}C atoms. A comprehensive description of the experiment as well as a comparison of the obtained results to those obtained from similar experiments carried out on AUG in 2003 and 2005 can be found in [1].

Reasons for the missing carbon can be various. For example, part of the ^{13}C may have been pumped out of the torus by cryopumps or it may have leaked from the injection valve to the vacuum pumps before being in contact with the plasma [1]. In addition, ^{13}C can be deposited in gaps between wall tiles. However, it is also likely that the deposition profile of ^{13}C is not entirely toroidally symmetric. Here, we present the first global 3D simulations of the performed experiment with the orbit-following Monte Carlo code ASCOT with the objective of addressing the issue of toroidal asymmetry.

Simulation parameters. The performed methane injection experiment was first modelled using the Monte Carlo impurity transport code DIVIMP [5]. The 2D background plasma was calculated with the onion-skin model (OSM, solver option 22) of the code, using Langmuir probe measurements of electron density and temperature at the inner and outer divertor targets as input data.

In the DIVIMP simulations, $^{13}C^{+}$ ions were initialized at the outer midplane and followed until they exited the calculation grid. The effects of erosion and re-deposition were not included in the DIVIMP cases. The studies showed that the simulations did not match the measured poloidal ^{13}C deposition profile when using the OSM-calculated deuteron flow field. Experimental measurements of plasma flow on various tokamaks have shown that the stagnation point of plasma flow is located somewhere between the outer midplane and the outer divertor in a configuration with the ion $\mathbf{B} \times \nabla B$ drift pointing towards the lower divertor [6, 7]. A reasonable match with the experimental results was found when a manually imposed deuteron flow field corresponding to these experimental observations was used, following the approach first presented in [8] and [9]. The DIVIMP modelling is described in more detail in [5].

Although the DIVIMP studies give an estimate of the large-scale deposition distribution in different poloidal regions, they do not provide any information of the toroidal deposition profile. For this reason, similar simulations were performed with the 3D Monte Carlo orbit-following code ASCOT [10].

The ASCOT code follows the orbits of individual test particles on steady-state magnetic and plasma backgrounds with accurately accounting for all neoclassical physics. The code can trace guiding centers, Larmor orbits and, in the case of neutrals, ballistic orbits in an unrestricted computational domain. Both the magnetic field and the wall geometry of the tokamak can be included in a realistic 3D form. Therefore, the code can address three-dimensional effects such as toroidal ripple and non-axisymmetric wall structures.

The effects of Coulomb collisions between the test particles and the background plasma are calculated using binomially distributed Monte Carlo operators derived from the Landau limit of the relativistic Balescu-Lenard collision operator for non-relativistic field particles [11]. The flow of the background plasma is taken into account by evaluating the collision operators in a frame of reference moving with the flow velocity. In addition to neoclassical physics, anomalous radial transport of test particles due to turbulence is modelled as diffusion.

For impurities, the effects of atomic reactions are calculated using a probabilistic model for effective ionization and recombination. The model updates the charge state of the test particle as it traverses in the background plasma based on reaction coefficients from the ADAS database for the local plasma conditions.

The previous DIVIMP simulations were used as a basis for the ASCOT modelling [5]. The background plasma solution from the DIVIMP OSM solver for the discharge #22575 was used for the scrape-off layer (SOL) plasma, excluding the plasma flow field. For the plasma flow, the imposed flow field from the DIVIMP studies was used. The imposed plasma flow field had a constant Mach number of $M = 0.5$ towards the divertors with a stagnation point roughly between the outer midplane and the outer divertor. As the employed DIVIMP grid did not extend to the wall, the halo plasma region between the SOL and the first wall was extrapolated manually. The halo plasma profiles of the ASCOT background plasma temperature, density and

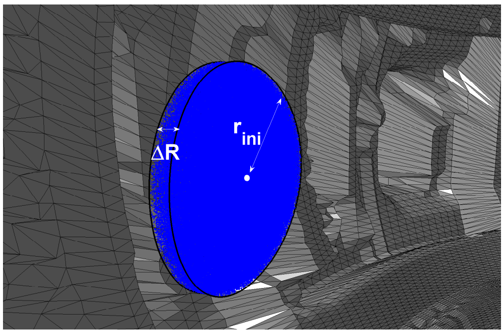

Figure 1. Illustration of the initial spatial distribution of $^{13}C^{+}$ ions (blue) in the ASCOT simulations.

flow velocity were extrapolated as exponentially decaying with the estimated decay lengths $\lambda_{T_e} = \lambda_{T_i} = 4$ cm, $\lambda_{n_e} = \lambda_{n_i} = 5$ cm and $\lambda_V = 5$ cm, respectively, that were chosen to approximately fit the temperature and density profiles and to provide a steeply decreasing flow profile. The assumption of exponentially decaying temperature and density profiles in the halo plasma has been experimentally verified in DIII-D [12] and AUG [13].

Experimental data from the same plasma discharge #22575 at 2.8 s was used to generate a magnetic field with toroidal ripple included. For the simulations, a realistic 3D wall geometry of ASDEX Upgrade was constructed based on a computer-aided design (CAD) data of the tokamak.

As ASCOT is not capable of following $^{13}CH_4$ molecules, the simulations were started with injecting $^{13}C^{+}$ ions. An ensemble of 300 000 ions was injected to sector 9 of AUG corresponding to the injection location in the experiment. The initial position of the particles was taken from a uniform random distribution over a cylindrical volume as visualized in figure 1. The volume extended radially $\Delta R = 5$ cm from the outer midplane separatrix towards the outer wall and $2 \cdot r_{ini} = 60$ cm in the toroidal direction, representing a large cloud of particles emerging from the injection valve.

The initialized carbon ions were given an initial energy of $E_0 = 0.3$ eV and a random pitch value ($\xi = v_{\|}/v$, where v is the total velocity and $v_{\|}$ the component parallel to the magnetic field) corresponding to an isotropic initial velocity distribution. The initial energy value is an average Franck-Condon energy of CH radicals. The anomalous radial diffusion coefficient was set to a constant value of $D_{\perp} = 0.25$ m^2/s. This was motivated by the observation that in the previous DIVIMP studies the best match with the experimental measurements was achieved with this particular value.

Simulation results. The ^{13}C deposition profile calculated with ASCOT, shown in figure 2(a), clearly indicates that the deposition in the main chamber is toroidally localized. Starting from their injection location in sector 9, the ^{13}C ions begin following the magnetic field lines in positive and negative toroidal directions. Near the outer midplane, protruding wall structures such as port and ICRH limiters collect substan-

Table 1. Comparison between the 2007 experiment [1] and ASCOT and DIVIMP [5] simulations of large-scale ^{13}C deposition. In the first row, the measured deposition, assuming toroidal symmetry, is normalized to the amount of injected ^{13}C. In the second row, the deposition is normalized to the amount of found ^{13}C with excluding the uncertain deposition at the top of the vessel. In the fourth and sixth rows, the same exclusion is applied for the modelling results. In addition to the shown regions, approximately 1.3 % of the injected atoms was found in remote areas in the experiment, mostly below the divertor roof baffle. The abbreviations are the same as in figure 2(a).

	ID	OD	OMP	PSL	Top	HS
Experiment (norm. to injected)	0.9 %	0.2 %	0.3 %	0.04 %	1 %	0.6 %
Experiment (norm. to found w/o top)	44 %	8 %	15 %	2 %	-	31 %
ASCOT	41 %	8 %	22 %	4 %	10 %	14 %
ASCOT (excluding top)	46 %	9 %	25 %	5 %	-	16 %
DIVIMP	31 %	5 %	10 %	4 %	23 %	27 %
DIVIMP (excluding top)	40 %	7 %	13 %	5 %	-	35 %

tial ^{13}C deposition and, consequently, the deposition profile is distinctively toroidally asymmetric in this region.

Driven by the background plasma flow, the carbon ions are strongly transported in the positive toroidal direction over the top of the vessel towards the inner divertor making the high-field side the dominant deposition region. It is noticeable that outside the outer midplane region (approximately $\theta \in [-64°, 44°]$), e.g., on the heat shield and in the divertor region, the deposition profile is rather symmetric toroidally. This can be explained by considering that the wall geometry in these regions is toroidally symmetric which, together with magnetic shear, results in a symmetric deposition profile.

A more concrete visualization of ^{13}C deposition in figure 2(b) shows that the injection valve is located betweed an ICRH limiter and a port limiter, leading to substantial deposition on these structures. From this view, the effect of different protruding wall structures around the torus on the deposition profile is evident. The figure also exemplifies the level of detail in the wall geometry of ASDEX Upgrade that was employed in the simulations.

The distribution of ^{13}C deposition in large-scale poloidal regions, presented in table 1, shows qualitative agreement with the experimental and DIVIMP results. However, the comparison is subject to uncertainty for multiple reasons and, consequently, should not be treated rigorously. First, the experimental results are based on only a small fraction of the injected ^{13}C that was found and the estimates of main chamber deposition are calculated from a very limited number of samples. In particular, this causes large uncertainty for the deposition at the top of the vessel which can reach a value of even 6 %. Therefore, the comparison to ASCOT and DIVIMP simulation results is most justified when the ^{13}C deposition is normalized to the amount of found ^{13}C and the uncertain deposition at the top is neglected. Second, it should be emphasized that

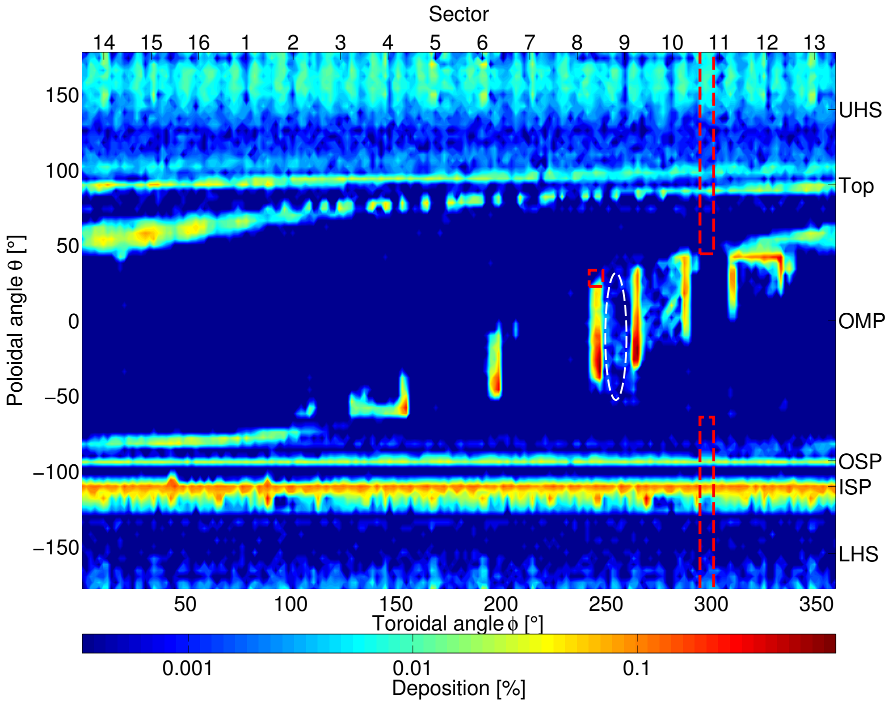

(a)

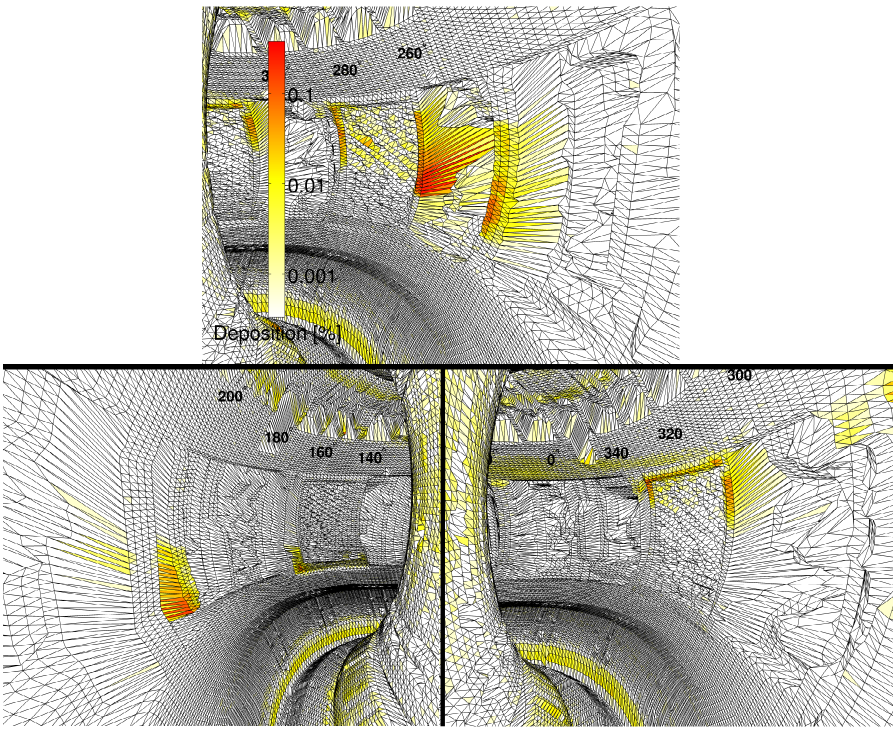

(b)

Figure 2. (a) 2D profile of ^{13}C deposition as calculated with ASCOT. The abbreviations used for different poloidal locations are “LHS” for the lower part of the heat shield, “ISP” for the inner strike point, “OSP” for the outer strike point, “OMP” for the outer midplane, “Top” for the top of the vessel and “UHS” for the upper part of the heat shield. Dashed red rectangles are drawn to indicate the approximate regions inside which wall tiles were removed for analysis after the experiment. The dashed white ellipse shows the location of the injection port. (b) 3D view of ^{13}C deposition on various parts of AUG: near the injection location in sector 9 (top), in sectors 4–6 (bottom left) and in sectors 12 and 13 (bottom right). The shown numbers indicate the toroidal angle corresponding to different sectors as shown in figure 2(a).

the DIVIMP results, in contrast to ASCOT, were achieved by varying the simulation parameters so that an as good as possible match with the experimental results was found.

A more quantitative estimate of the effect of toroidal asymmetry can be obtained from the following calculation. First, ^{13}C deposition inside the regions where the wall tiles were removed after the experiment is calculated, see figure 2(a). The number of deposited particles is then integrated toroidally around the torus to obtain the total deposition in the same manner as performed for the experimental data. In this calculation, the small sampled region in sector 8 is integrated poloidally over the outer midplane region to obtain an estimate of the deposition there. As a result, the described calculation estimates that the total number of deposited ^{13}C particles is approximately 70 % of the number of injected ^{13}C ions. Therefore, it can be concluded that, in this particular case, assuming toroidally symmetric deposition would cause 30 % of the injected ^{13}C not to be accounted for.

Sensitivity analysis of the simulation parameters proved that the main results of the deposition profiles are robust. The anomalous radial diffusion coeffiecient $D_\perp$ was varied in the range 0.1 m^2/s–1.0 m^2/s and the the radial extent of the initial spatial distribution of the injected ^{13}C ions, the parameter ΔR, was varied between 1 cm and 9 cm. Increasing values of $D_\perp$ and ΔR were observed to shift deposition from the divertor region towards the main chamber with, however, maintaining the qualitative structure of the deposition profiles. The effect of the initial energy E_0 of the injected carbon ions on the deposition profile was found to be weak. With values of E_0 between 0.1 eV and 20 eV, it was observed that the effect of the background plasma flow slightly decreases with increasing E_0. In practice, ^{13}C deposition decreased in the direction of the plasma flow which, near the injection location, is poloidally towards the inner divertor and toroidally in the positive direction (counter-clockwise when viewed from above). The halo plasma profiles (values for the decay lengths λ, varied in the range approximately 2–5 cm) mostly affected deposition at the top of the vessel, where the gap between the DIVIMP grid and the wall is the largest. This did not, however, alter the conclusions.

The effect of reflection from wall surfaces was studied with a simple model that uses a constant sticking coefficient. In the model, each time a test particle encounters a wall surface, it is reflected back into the plasma with a predefined, constant probability. The particles are reflected as neutrals with their energy corresponding to their impact energy and with a random direction of velocity. It was observed that, even with a low sticking coefficient, local re-deposition of the reflected particles was dominant and the 2D deposition pattern only became slightly more diffuse, in particular around the protruding wall structures near the outer midplane. The result can be considered to give a qualitative indication of the effect of erosion of deposited particles on the deposition pattern. This and the performed sensitivity analysis proved that the presented features of the toroidal profile, strong asymmetry near the outer midplane and symmetry in other regions, remain unchanged over a wide range of different simulation parameters.

Discussion and conclusions. The presented ASCOT simulation results show that non-axisymmetric wall geometry can have a large impact on impurity transport. They can provide a partial explanation to why only approximately 4.5–9.5 % of the injected ^{13}C could be accounted for in the 2007 experiment in ASDEX Upgrade when deposition was assumed toroidally symmetric. However, discrepancies in the large-scale deposition results between the experiment and simulations were observed. It should be stressed that the presented ASCOT simulations used a manually imposed background plasma flow profile. The transport of ^{13}C has been observed to be very sensitive to changes in the flow profile [5]. It is, therefore, the background plasma that predominantly determines the global carbon transport. Nevertheless, we have verified that this does not cancel the shown effect of non-axisymmetric wall geometry.

In the view of the obtained results, it is of interest to refer to similar experiments carried out on DIII-D [3, 8, 9, 14, 15, 16]. In these experiments, $^{13}CH_4$ was injected into the torus in a toroidally symmetric manner from the top of the vessel. In this case, the assumption of toroidally symmetric ^{13}C deposition is more justified than when using only one injection valve. This is, at least partially, due to the fact that the effect of protruding wall structures on the deposition profile is distributed more evenly around the entire torus when using toroidally symmetric injection. Supportive of the presented argument, up to approximately 50 % of the injected ^{13}C was accounted for in post mortem analysis when ^{13}C deposition was assumed toroidally symmetric in the DIII-D experiments.

In the presented ASCOT simulations, the effects of the thermal force, reflection from wall surfaces, erosion of deposited test particles and electric fields were neglected. In order to provide more quantitative simulations of impurity migration, the code is being upgraded to include the effects of these phenomena. It is possible, e.g., that erosion of deposited ^{13}C would lead to increased re-deposition in areas shadowed from direct plasma contact.

A new $^{13}CH_4$ injection experiment was conducted on ASDEX Upgrade in 2011. For the experiment, predictive ASCOT modelling was carried out using a new 3D wall geometry that takes into account even the most recent changes in AUG such as structures due to resonant magnetic perturbation coils. Strong toroidal asymmetry was observed in the simulation results, similarly as presented here. Preliminary experimental results have shown confirmation of the predicted effect of non-axisymmetric wall geometry. In the first analyzed samples, strong ^{13}C deposition peaks were observed on ICRH antenna structures as well as on wall tiles next to the injection port with ^{13}C surface densities reaching 10^{17}–10^{18} at/cm^2. Significant asymmetry in deposition was also noticed between antennas separated toroidally by 180 degrees. A more detailed analysis of the results will be presented in [17]. In addition to the investigation of toroidal asymmetry, deposition in gaps between adjacent tiles will be studied.

This work, supported by the European Communities under the contract of Association between Euratom and Tekes, was carried out within the framework of the Task Force on Plasma Wall Interactions of the European Fusion Development Agreement. The views and opinions expressed herein do not necessarily reflect those of the European Commission. This work was partially supported by the Academy of Finland projects No. 121371 and 134924. The supercomputing resources of CSC – IT center for science were utilized in the studies.

References

[1] A. Hakola, J. Likonen, L. Aho-Mantila, M. Groth, S. Koivuranta, K. Krieger, T. Kurki-Suonio, T. Makkonen, M. Mayer, H.W. Müller, R. Neu, V. Rohde, and the ASDEX Upgrade Team. Migration and deposition of ^{13}C in the full-tungsten ASDEX Upgrade tokamak. *Plasma Physics and Controlled Fusion*, 52(6):065006, 2010.

[2] A. Loarte, B. Lipschultz, A.S. Kukushkin, G.F. Matthews, P.C. Stangeby, N. Asakura, G.F. Counsell, G. Federici, A. Kallenbach, K. Krieger, A. Mahdavi, V. Philipps, D. Reiter, J. Roth, J. Strachan, D. Whyte, R. Doerner, T. Eich, W. Fundamenski, A. Herrmann, M. Fenstermacher, P. Ghendrih, M. Groth, A. Kirschner, S. Konoshima, B. LaBombard, P. Lang, A.W. Leonard, P. Monier-Garbet, R. Neu, H. Pacher, B. Pegourie, R.A. Pitts, S. Takamura, J. Terry, E. Tsitrone, the ITPA Scrape-off Layer, and Divertor Physics Topical Group. Chapter 4: Power and particle control. *Nuclear Fusion*, 47(6):S203, 2007. Progress in the ITER Physics Basis.

[3] S.L. Allen, W.R. Wampler, A.G. McLean, D.G. Whyte, W.P. West, P.C. Stangeby, N.H. Brooks, D.L. Rudakov, V. Phillips, M. Rubel, G.F. Matthews, A. Nagy, R. Ellis, and A.S. Bozek. ^{13}C transport studies in L-mode divertor plasmas on DIII-D. *Journal of Nuclear Materials*, 337–339:30–34, 2005.

[4] J.P. Coad, J. Likonen, M. Rubel, E. Vainonen-Ahlgren, D.E. Hole, T. Sajavaara, T. Renvall, G.F. Matthews, and JET EFDA Contributors. Overview of material re-deposition and fuel retention studies at JET with the Gas Box divertor. *Nuclear Fusion*, 46(2):350, 2006.

[5] T. Makkonen, M. Groth, T. Kurki-Suonio, K. Krieger, L. Aho-Mantila, A. Hakola, J. Likonen, and H.W. Müller. DIVIMP simulations of ^{13}C puffing experiments in ASDEX Upgrade L-mode plasma. *Journal of Nuclear Materials*, 415:S479–S482, 2011.

[6] Nobuyuki Asakura and ITPA SOL and Divertor Topical Group. Understanding the SOL flow in L-mode plasma on divertor tokamaks, and its influence on the plasma transport. *Journal of Nuclear Materials*, 363–365:41–51, 2007.

[7] B. Lipschultz, X. Bonnin, G. Counsell, A. Kallenbach, A. Kukushkin, K. Krieger, A. Leonard, A. Loarte, R. Neu, R.A. Pitts, T. Rognlien, J. Roth, C. Skinner, J.L. Terry, E. Tsitrone, D. Whyte, S. Zweben, N. Asakura, D. Coster, R. Doerner, R. Dux, G. Federici, M. Fenstermacher, W. Fundamenski, P. Ghendrih, A. Herrmann, J. Hu, S. Krasheninnikov, G. Kirnev, A. Kreter, V. Kurnaev, B. LaBombard, S. Lisgo, T. Nakano, N. Ohno, H.D. Pacher, J. Paley, Y. Pan, G. Pautasso, V. Philipps, V. Rohde, D. Rudakov, P. Stangeby, S. Takamura, T. Tanabe, Y. Yang, and S. Zhu. Plasma-surface interaction, scrape-off layer and divertor physics: implications for ITER. *Nuclear Fusion*, 47(9):1189, 2007.

[8] A.G. McLean, J.D. Elder, P.C. Stangeby, S.L. Allen, J.A. Boedo, N.H. Brooks, M.E. Fenstermacher, M. Groth, S. Lisgo, A. Nagy, D.L. Rudakov, W.R. Wampler, J.G. Watkins, W.P. West, and D.G. Whyte. DIVIMP modeling of the toroidally symmetrical injection of $^{13}CH_4$ into the upper SOL of DIII-D. *Journal of Nuclear Materials*, 337-339:124–128, 2005.

[9] J.D. Elder, A.G. McLean, P.C. Stangeby, S.L. Allen, J.A. Boedo, B.D. Bray, N.H. Brooks, M.E. Fenstermacher, M. Groth, A.W. Leonard, D. Reiter, D.L. Rudakov, W.R. Wampler, J.G. Watkins, W.P. West, and D.G. Whyte. OEDGE modeling of the DIII-D H-mode $^{13}CH_4$ puffing experiment. *Journal of Nuclear Materials*, 363-365:140–145, 2007.

[10] Seppo Sipilä. *Monte Carlo simulation of charged particle orbits in the presence of radiofrequency waves in tokamak plasmas.* PhD thesis, Helsinki University of Technology, 1997.

[11] A. H. Boozer and G. Kuo-Petravic. Monte Carlo evaluation of transport coefficients. *Physics of Fluids*, 24(5):851–859, 1981.

[12] D.L. Rudakov, J.A. Boedo, R.A. Moyer, P.C. Stangeby, J.G. Watkins, D.G. Whyte, L. Zeng,

N.H. Brooks, R.P. Doerner, T.E. Evans, M.E. Fenstermacher, M. Groth, E.M. Hollmann, S.I. Krasheninnikov, C.J. Lasnier, A.W. Leonard, M.A. Mahdavi, G.R. McKee, A.G. McLean, A.Yu. Pigarov, W.R. Wampler, G. Wang, W.P. West, and C.P.C. Wong. Far SOL transport and main wall plasma interaction in DIII-D. *Nuclear Fusion*, 45(12):1589, 2005.

[13] H.W. Müller, V. Bobkov, G. Haas, M. Jakobi, M. Laux, M. Maraschek, J. Neuhauser, M. Reich, V. Rohde, J. Schweinzer, E. Wolfrum, and ASDEX Upgrade Team. Profile and Transport Studies in the outer Scrape Off Layer at ASDEX Upgrade. *Europhysics Conference Abstracts*, 26B:O–2.06, 2002.

[14] W.R. Wampler, A.G. McLean, S.L. Allen, N.H. Brooks, J.D. Elder, M.E. Fenstermacher, M. Groth, P.C. Stangeby, W.P. West, and D.G. Whyte. Transport and deposition of 13C from methane injection into partially detached H-mode plasmas in DIII-D. *Journal of Nuclear Materials*, 363–365:72–77, 2007.

[15] J.D. Elder, A.G. McLean, P.C. Stangeby, S.L. Allen, J.A. Boedo, B.D. Bray, N.H. Brooks, M.E. Fenstermacher, M. Groth, A.W. Leonard, D.L. Rudakov, W.R. Wampler, J.G. Watkins, W.P. West, and D.G. Whyte. Indications of an inward pinch in the inner SOL of DIII-D from ^{13}C deposition experiments. *Journal of Nuclear Materials*, 390–391:376–379, 2009.

[16] J.D. Elder, W.R. Wampler, A.G. McLean, P.C. Stangeby, S.L. Allen, B.D. Bray, N.H. Brooks, A.W. Leonard, E.A. Unterberg, and J.G. Watkins. OEDGE modeling of the DIII-D double null puffing experiment. *Journal of Nuclear Materials*, 415:S513–S516, 2011.

[17] A. Hakola, S. Koivuranta, J. Likonen, M. Groth, T. Kurki-Suonio, V. Lindholm, T. Makkonen, J. Miettunen, K. Krieger, M. Mayer, H.W. Müller, R. Neu, V. Rohde, P. Petersson, and ASDEX Upgrade Team. Global migration of ^{13}C and ^{15}N in high-density L-mode plasmas at ASDEX Upgrade. to be presented in 20th International Conference on Plasma Surface Interactions (21–25 May 2012, Aachen, Germany).